Available online at www.sciencedirect.com
ScienceDirect
Progress in Natural Science 19 (2009) 479–487
Progress in Natural Science
www.elsevier.com/locate/pnsc

Fluorescence detection and imaging of cytosolic calcium oscillations: A comparison of four equipment setups

Xiaofeng Fang [a,1], Xiaoting Zhao [a,1], Wei Zhou [a], Jia Li [a], Qin Liu [a], Xun Shen [b], Yoh-ichi Satoh [c], Zong Jie Cui [a,*]

[a] *Institute of Cell Biology, Beijing Normal University, Beijing 100875, China*
[b] *Institute of Biophysics, Chinese Academy of Sciences, Beijing 100101, China*
[c] *Department of Histology, Iwate Medical University School of Medicine, Uchimaru 19-1, Morioka 020-8505, Japan*

Received 8 April 2008; received in revised form 7 May 2008; accepted 28 May 2008

Abstract

The increase in cytosolic calcium concentration has been shown to play an important role in vital cellular functions such as muscle contraction, cell secretion, oocyte fertilization, nerve conduction, embryo development and apoptosis in animals, plants and microbes, and in the invasion of mammalian cells by parasites, bacteria, and viruses. Therefore, live cell imaging of increases in cytosolic calcium concentration in cellular compartments has been investigated intensively. Multiple calcium imaging systems are now available commercially, but when it comes to deciding which model to purchase, it is often hard to obtain enough information for an optimal setup. In this paper, a comparison was made among four fluorescent detection/imaging devices for the detection of cytosolic calcium oscillations induced in rat pancreatic acinar cells by cholecystokinin and in hepatocytes by phenylephrine. Detailed equipment setup, differences in data acquisition and analysis, and side effects of the excitation light on live cells were analyzed. A list of important factors that should be considered in choosing the optimal equipment are recommended, which will be useful for users of such devices in the future.

Keywords: Calcium measurement system; Pancreatic acinar cells; Hepatocytes; Cytosolic calcium oscillations

1. Introduction

Increase in cytosolic calcium concentration is pivotal in the regulation of muscle contraction, cell secretion, fertilization, neural transmission, embryo development, and apoptosis [1–3]. Calcium signaling has been found to be vital in the normal functioning of animals, plants, and microbes [4–7], and has been found to play important roles in mammalian cell invasion by parasites, bacteria, and viruses [8–10]. Imaging of increases in cytosolic calcium concentration within subcellular compartments in living cells has been intensively investigated. The time-scan mode of laser confocal microscopy has been used for calcium imaging. However, more detailed investigations require the use of a dedicated calcium imaging system, especially if the investigation takes place over an extended period of time. Although multiple commercial suppliers are able to provide such measuring devices, detailed technical information is often not provided, especially in regard to specific applications. The modular design of some imaging devices allows users to have multiple options, but an ordinary user is often not fully aware of its full potential when selecting or specifying the different components, making the purchasing process difficult. In this paper, we compared in detail four fluorescent calcium measurement and imaging systems, and used these systems to measure oscillatory increases in calcium concentration in

* Corresponding author. Tel./fax: +86 10 58809162.
E-mail address: zjcui@bnu.edu.cn (Z.J. Cui).
[1] The authors contributed equally to this work.

1002-0071/$ - see front matter
doi:10.1016/j.pnsc.2008.05.037

freshly isolated rat pancreatic acinar cells and hepatocytes. We hope that such comparative studies will be useful to investigators who are planning to buy a fluorescent calcium measurement/imaging system, and may provide some useful hints for the manufacturers also.

As noted above, multiple types of cells after stimulation show regularly interspaced increases in cytosolic calcium concentration. Such oscillatory increases in cytosolic calcium concentration are commonly found after stimulation with low physiological concentrations of acetylcholine (ACh) or cholecystokinin (CCK) in the pancreatic acinar cells [11–15]. Similarly, rat hepatocytes when stimulated with physiological concentrations of noradrenaline (NE), vasopressin (VP), or angiotensin also show typical cytosolic calcium oscillations [16–19]. In this paper, these two types of cells will be investigated.

A large selection of fluorescent calcium indicators can be used for calcium imaging. When a conventional confocal laser scanning microscope is used for calcium imaging, fluorescent indicators excitable with visible light are often used. This is mainly because most confocal microscopes are not equipped with lasers emitting in the UV region. Therefore, it is not possible to use dual wavelength indicators excitable with UV light, such as Fura-2. Instead, single wavelength indicators such as Fluo-3 are used. The problem with single wavelength indicator imaging is that the fluorescent intensity distribution within a cell could be a simple reflection of indicator concentration instead of the differences in calcium concentration. With dual wavelength probes, there is no such problem because the corresponding ratio would cancel out any such artifacts. In this paper, the dual wavelength probe Fura-2 was used for calcium measurement and imaging.

2. Materials and methods

2.1. Reagents

Cholecystokinin octa-peptide (CCK-8), bovine serum albumin (BSA), soybean trypsin inhibitor, and phenylephrine (PE) were products of Sigma–Aldrich (St. Louis, MO, USA). Collagenase P and H, and 4-(2-hydroxyethyl)-1-piperazineethane-sulfonic acid (Hepes) were from Roche (Mannheim, Germany), and MEM amino acids mixture was from GIBCO-BRL (Grand island, NY, USA). Fura-2 AM was from Molecular Probes (Eugene, OR, USA), and Cell-Tak was purchased from BD Biosciences (Bedford, MA, USA).

2.2. Isolation of rat pancreatic acinar cells

Rat pancreatic acinar cells were prepared as reported [12,14]. Male Sprague–Dawley rats (Vital River Experimental Animals, Beijing) weighing approximately 250–350 g were killed by cervical dislocation. The pancreas was excised and digested in 5 ml collagenase P (800 U in 10 ml buffer) at 37 °C, with shaking at 120 rpm for 40 min. The digested tissue was then dispersed and filtered using a nylon mesh (150 mesh) in Kreb's buffer containing BSA 4% [12]. The Kreb's buffer used had the following compositions (in mM): NaCl 118, KCl 4.7, $CaCl_2$ 2.5, $MgCl_2$ 1.13, NaH_2PO_4 1.0, D-glucose 5.5, Hepes 10, l-glutamine 2.0, bovine serum albumin (BSA) 2 g l^{-1}, MEM amino acids mixture 2%, soybean trypsin inhibitor 0.1 g l^{-1}, with pH adjusted to 7.4 with NaOH 4 M. Buffer was oxygenated for 30 min before use. The use of Kreb's buffer for cell perfusion eliminated the need for glutamine, BSA, amino acid mixture, and trypsin inhibitors.

2.3. Isolation of rat hepatocytes

Rat hepatocytes were isolated as reported [18,19]. Rat of the SD strain was killed, portal vein cannulated and perfused at 30 ml min^{-1} with 150 ml of divalent cation-free buffer, followed by perfusion with 80 ml of buffer containing collagenase. After perfusion, the softened tissue was excised, and further incubated for 2 min in a shaking water bath. Dispersed hepatocytes were filtered through a nylon mesh (150 mesh) into a buffer containing BSA 3 g l^{-1}, and washed 3 times. The buffer used for the isolation was as follows (mM): NaCl 118, KCl 4.7, $CaCl_2$ 2.5, $MgCl_2$ 1.13, NaH_2PO_4 1, D-glucose 5.6, Hepes 10, L-glutamine 2, sodium pyruvate 2, BSA 2 g l^{-1}, MEM amino acids (×50) 2%, pH was adjusted to 7.4. For hepatocytes perfusion, BSA, amino acids mixture, sodium pyruvate and L-glutamine were omitted.

2.4. Measurement of calcium concentration

Freshly isolated rat pancreatic acinar cells or hepatocytes were loaded with Fura-2 AM (final concentration 5 μM) in a shaking water bath at 37 °C for 30 min. Fura-2 AM-loaded cells were attached to Cell-Tak-coated cover-slips assembled into Sykes-Moore perfusion chambers and placed on the platform of an inverted fluorescent microscope. Fura-2 fluorescence in the selected regions of interests (ROIs) was measured.

2.5. Equipment setups for fluorescence calcium measurement and imaging

Four different equipment setups used to measure cytosolic calcium signals are indicated in Fig. 1. Each part of the four systems is shown in Fig. 1(a); Fig. 1(b) indicates the corresponding components, Fig. 1(c) and (d) shows the emission spectrum of the metal halide lamp used in System I (Fig. 1(c)), and of the xenon lamp used in Systems II–IV (Fig. 1(d)).

2.5.1. System I

As indicated in Fig. 1, the light source used for System I was a Lumen 200 Pro from Prior Scientific Inc. (Fulbourn, Cambridge, UK), with a metal halide lamp. Its emission spectrum covers 350–650 nm, with a power

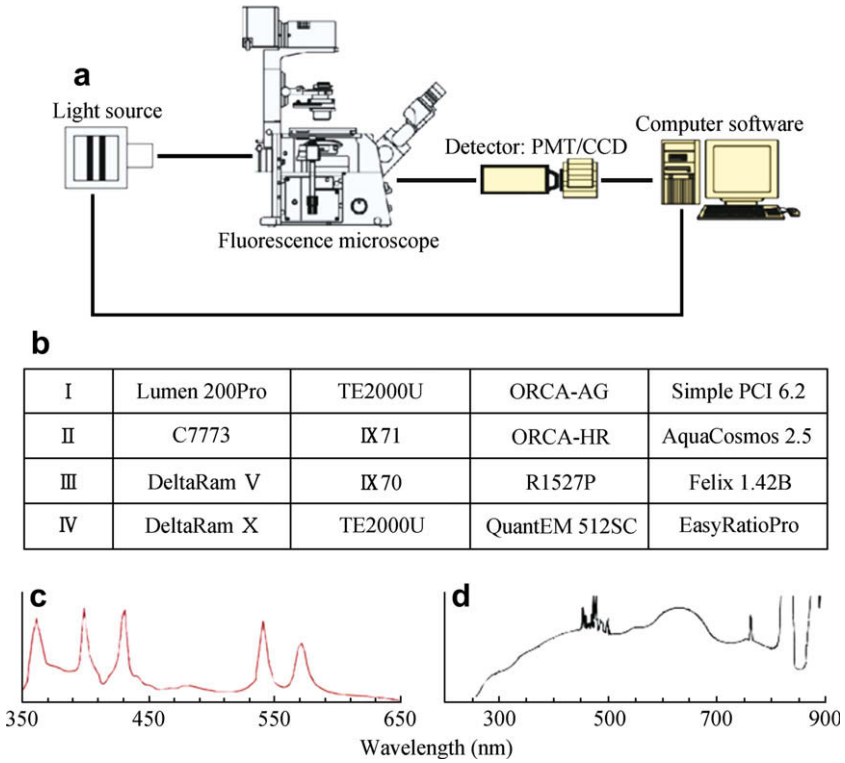

I	Lumen 200Pro	TE2000U	ORCA-AG	Simple PCI 6.2
II	C7773	IX71	ORCA-HR	AquaCosmos 2.5
III	DeltaRam V	IX70	R1527P	Felix 1.42B
IV	DeltaRam X	TE2000U	QuantEM 512SC	EasyRatioPro

Fig. 1. Composition of the calcium measurement systems. (a) Each system is composed of an independent light source, an inverted fluorescence microscope, emitted photon detector (PMT/CCD), and a computer and software. (b) Details of each component of the Systems I–IV: light sources were from Prior Scientific (I), Hamamatsu (II), PTI (III and IV); microscopes were from Nikon (I), Olympus (II and III), Nikon (IV); detectors were Hamamatsu CCD ORCA-AG (I) and ORCA-HR (C4742-95-12HR) (II), Hamamatsu PMT R1527P (III), Roper Scientific CCD QuantEM 512SC (IV); softwares used were Hamamatsu/Compix Inc. Simple PCI 6.2 (I), Hamamatsu AquaCosmos (II), PTI Felix 1.42B (III) and EasyRaioPro (IV). PTI: Photon Technology International. (c) and (d) Emission spectrum of light sources for Systems I–IV. (c) Metal halide lamp (Lumen 200 Pro of System I); (d) xenon lamp (Hamamatsu C7773 of System II, DeltaRam V/X of Systems III and IV). Lamp emission information was from respective websites (Prior Scientific Inc.: http://www.prior.com/downloads/user_files/en/Lumen200PRO_Datasheet.pdf; Photon Technology International: http://www.pti-nj.com/UVvis/UVHardware.html).

output of 200 W and a lamp life of 2000 h (mercury lamps of 100 W normally have a lamp life of 300 h). Lumen 200 Pro has a built-in motor-driven six-positioned filter wheel (diameter 25 mm); switching between neighboring-filters (340 and 380, for example) is rapid, and is completed within 55 ms. A shutter control facilitates graded power output; an outside control enables manual switching. Filtered light from Lumen 200 Pro is transmitted to the fluorescent microscope via a 2 m long liquid light guide, to avoid heat and vibration transmission to the microscope.

The microscope used for System I was Nikon TE-2000U (Nikon, Japan), which was equipped with a Fura-2 filter set (Chroma 74500 – with a dichroic mirror and an emission filter, the excitation filter being placed in the filter wheel in Lumen 200 Pro). TE-2000U was equipped with a fluorescent objective 40× (oil), which has 52% transmission at 340 nm and 74% at 380 nm. The detector in System I was a CCD camera (ORCA-AG, Hamamatsu, Japan). ORCA-AG has pixels of 1344 × 1204, and is cooled to −30 °C, and has a quantum yield of 70% from 470 to 570 nm.

The data acquisition and analysis software used in System I was Simple PCI 6.2 (Hamamatsu/Compix Inc.). This software has a modular design, and in this work the following modules were used: AIC, automated image capture and multi-dimensional visualizer which includes a CCD camera driver, a standard and advanced equipment driver, and an experiment planner; IPA, image processing and analysis; DIA, dynamic intensity analysis, which can analyze topical density, calcium concentration, dual wavelength ratio, pH ratio measurement; and DNN, de-blurring and restorative algorithms.

2.5.2. System II

System II (Fig. 1) was equipped with a high-speed scanning monochromater (Hamamatsu C7773), with a switching speed for 340/380 nm of 3 ms. The xenon lamp used was 150 W.

An Olympus IX71 inverted fluorescence microscope was used in System II. The objective used most often was UAPO40X3/340. Detector of emitted light was Hamamatsu CCD ORCA-HR (C4742-95-12HR) with pixels of 4000 × 2624, the shortest exposure time was 330 s, making it most suitable for high-speed imaging of weak signals.

AquaCosmos 2.5 (Hamamatsu, Japan) was used for data acquisition and analysis. Online display of images for 340 and 380 nm, and for F340/F380, was possible, together with fluorescence intensity display. New ROIs could be drawn, and time course was analyzed after the completion of the experiment.

2.5.3. System III

System III (Fig. 1) was equipped with monochromater DeltaRam V from PTI, with a xenon lamp of 75 W. The power output at a certain wavelength could be as high as 19 mW (see Section 4). The wavelength switching speed of DeltaRam V could reach 80 nm/s.

An inverted fluorescence microscope (Olympus IX-70) was used, which was equipped with a Fura-2 filter set. Emitted light was detected by Hamamatsu PMT R1527P (PMT814, PTI), which could be operated in analog or digital mode (photon counting mode), with detection from 200 to 680 nm.

Data acquisition/analysis software for System III was Felix 1.42B, with an online display of fluorescence intensities at 340 and 380 nm, and ratio F340/F380.

2.5.4. System IV

The light source in System IV (Fig. 1) was monochromater DeltaRam X from PTI. A xenon lamp of 75 W was used, without cooling, and no ozone was produced. Multiple wavelength scan from 250 to 680 nm was possible with DeltaRam X. Similar to DeltaRam V, DeltaRam X also has double adjustable slits, adjustable from 0 to 24 nm. Switching between 340 and 380 nm for DeltaRam V can be completed in less than 2 ms, and a complete change among four different wavelengths could be made within 15 ms.

Similar to System I, a Nikon TE-2000U (Nikon, Japan) was used in System IV. The objective Super Fluor 40× has a transmission of 43% at 340 nm. Because a monochromater was used as the light source, the excitation filter for the Fura-2 filter set (Systems II–IV) could be omitted; whereas in System I, the excitations filters for 340 and 380 nm were inserted into the filter wheel in Lumen Pro 200. The detector for System IV was a CCD from Roper Scientific (QuantEM 512 CS), with tandem amplifiers and cooling temperature to −30 °C, and a quantum yield of >90%. EasyRatioPro from PTI was used for data acquisition and analysis. A fashionable WarpDrive makes computer mouse operations redundant. Real time fluorescent images at 340 nm, 380 nm, and ratio images F340/F380 could be displayed, as well as fluorescence intensity plot for different ROIs.

Tables 1 and 2 list the major characteristics of the light sources and detectors used in this work.

3. Results

3.1. System I

Fig. 2(a) shows a bright field image of rat pancreatic acini taken with System I. The micrograph shows clearly defined acinar cell profiles, a zymogen granule-rich apical portion and a clear basolateral portion. The green-outlined ROIs are: ROI 1.1 – an entire acinar cell on the right side, ROI 1.2 – basal, ROI 1.3 – the granule-rich apical portion of the acinar cell, which represents the average calcium concentration within these three ROIs, respectively (Fig. 2(b)). CCK (10 pM) induced regular calcium oscillations in the selected pancreatic acinar cell. The onset of calcium spikes was different at different locations in the same cell. In the early stages of stimulation, calcium spikes appeared first in the apical portion; but at the later stages, calcium spikes appeared first in the basal portion. The amplitude of the spike was also different in different portions of the acinar cell. The spike was obviously higher in the basal than that on the apical side. Although the overall oscillatory frequency was similar in apical and basal portions, the smaller spikes which appeared in the apical portion during early stimulation were not seen in the basal portion (Fig. 2(c)).

Table 1
Characteristics of the light sources.

System	Name	Lamp (W)	Category	Emission peaks range (nm)	Switching speed (340/380 nm) (ms)	Monochromatic light band width (nm)/power (mW)
I	Lumen Pro200	Metal halide (200)	Filter wheel	360, 400, 430, 540, 570	55	25/–
II	C7773	Xenon (150)	Monochromater	330–650	3	Adjustable/3.5 (at 500 nm)
III	DeltaRam V	Xenon (75)	Monochromater	250–680	2	0–24/-
IV	DeltaRam X	Xenon (75)	Monochromater	250–680	2	0–24/19 (at 473 nm)

Table 2
Characteristics of the detectors.

System	Name	Category	Exposure time/readout speed	Quantum efficiency (%)	Pixels	Cooling temperature (°C)
I	ORCA-AG	CCD	10 (μs)– 4200 (s)	70	1344 × 1204	−30
II	ORCA-HR	CCD	330 (μs)– 10 (s)	50	4000 × 2624	5–7
III	1527P	PMT	–	10–20	–	–
IV	QuantEM512SC	CCD	1.5–10 (MHz)	90	512 × 512	−30

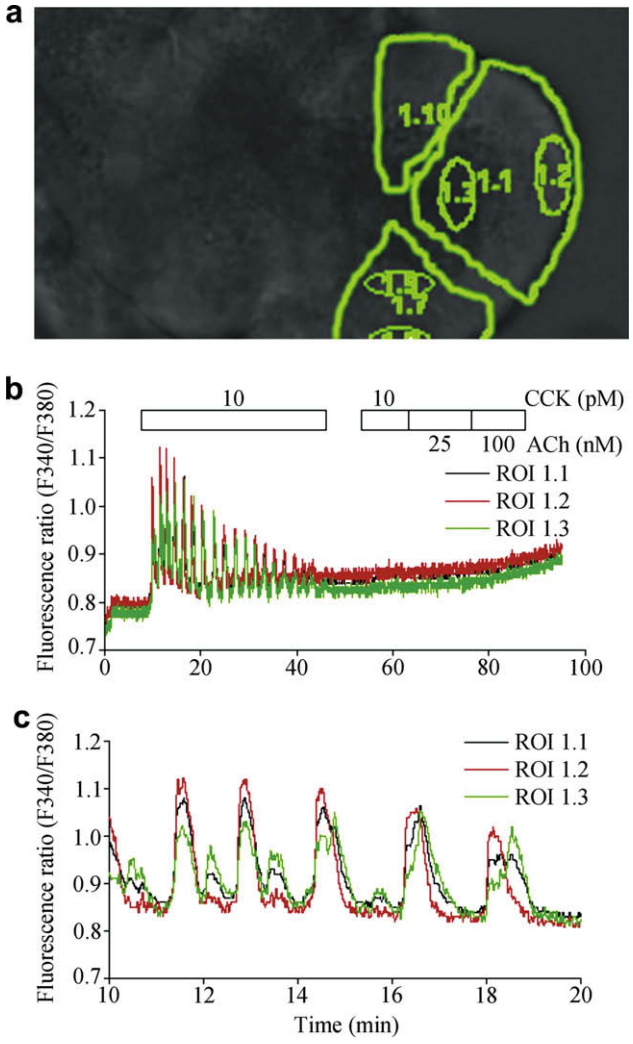

Fig. 2. Calcium oscillations detected in rat pancreatic acinar cells with System I. (a) A phase contrast micrograph of pancreatic acini, ROIs 1.1–1.3 represent a whole cell, basal portion of the cell, and apical portion of the acinar cell, respectively. (b) Cytosolic calcium concentration changes with time after stimulation with 10 pM CCK 25 and 100 nM ACh in ROIs 1.1–1.3. (c) An enlargement of a portion of the trace in (b). The horizontal bars in (b) indicate time of drug application.

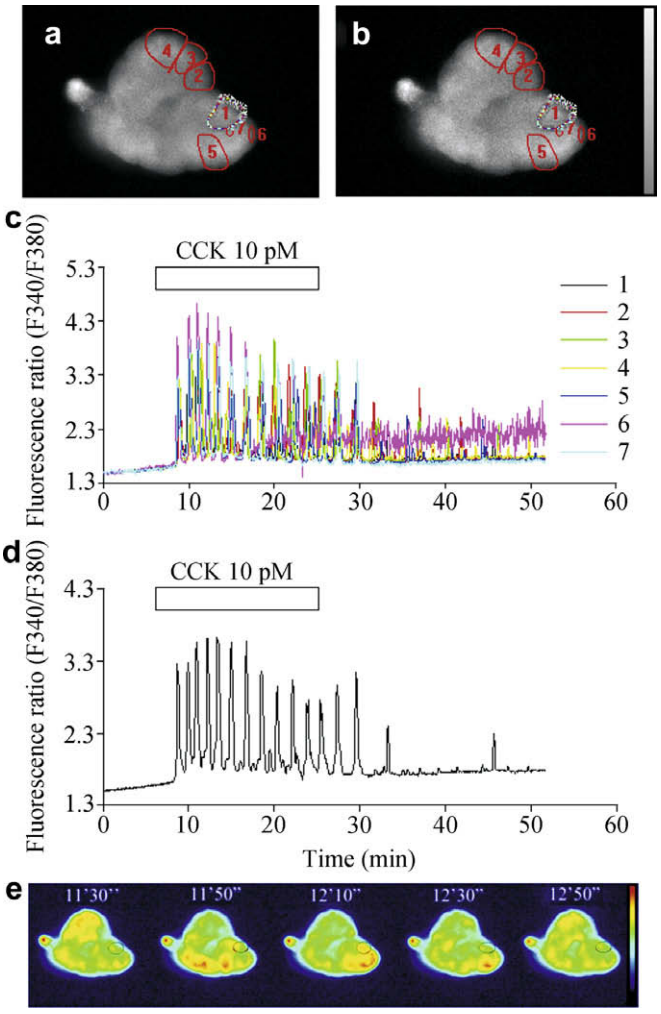

Fig. 3. Oscillatory increases in cytosolic calcium concentration in rat pancreatic acinar cells detected in System II. (a) and (b) Fluorescence images of Fura-2-loaded rat pancreatic acinar cells with excitations at 340 nm (a) and 380 nm (b). ROIs 1–7 are as indicated. The grey scale bar on the right indicates fluorescence intensity with excitations at 340 and 380 nm. (c) Oscillatory increases in cytosolic calcium concentration in ROIs 1–7 after stimulation with 10 pM CCK. (d) Trace indicates calcium concentration changes in ROI 1. (e) Fluorescence images with 340 nm excitation in ROI 1 (annotated cell in (a) and (b)), at indicated time points, note that compared with time point 11′30″, the fluorescence intensity in ROI 1 at 11′50″ and 12′10″ was significantly brighter, with fluorescence intensity returning to basal level at 12′30″ and 12′50″. The pseudo-color scale bar on right indicates F340 fluorescence intensity. The horizontal bars in (c) and (d) indicate time of CCK application.

The oscillatory calcium signals in those different ROIs decayed gradually with time. After wash-off of CCK, re-addition of 10 pM CCK, 25 nM ACh, 100 nM ACh all failed to induce any further increase in cytosolic calcium concentration (Fig. 2(b), $n = 6$).

3.2. System II

Similarly, in System II, it was also found that 10 pM CCK stimulation of pancreatic acinar cells induced regular calcium oscillations in different acinar cells (Fig. 3(a) and (b)); the amplitude of calcium spikes was similar, and oscillations disappeared after wash-out of CCK (Fig. 3(c) and (d), $n = 7$). In System II, fluorescent images of 340 nm excitation, 380 excitation, and ratio (340/380 nm) images, as well as time-course plots of the corresponding fluorescence intensities for each ROI, could all be shown online, in separate windows. The pseudo-color codes indicate real time changes in calcium concentration (Fig. 3(e)).

Judging from Fig. 3 it was apparent that calcium oscillations in different acinar cells in the same acinus were not synchronized, the oscillatory frequency and amplitude were all different for each cell (see ROI 6 and ROI 7 in Fig. 3(c)). The amplitude was larger in the basal portion. Fig. 3(d) indicates calcium changes with time in ROI 1; Fig. 3(e) shows such changes in F340 from 11′30″ to 12′50″ in ROI 1.

3.3. System III

In System III, only one cell could be examined at a time, because only one ROI could be selected by the pin-hole device (Fig. 4(a)). With the pin-hole device, one can manually select one cell or one ROI in the field of view by adjusting the position of four sides of the ROI. As shown in Fig. 4(b), 5 pM CCK induced persistent calcium oscillations in a stimulated pancreatic acinar cell; and wash-out of CCK resulted in the disappearance of the calcium oscillations (Fig. 4(b)). Since only one ROI can be measured at a time, parallel experiments with multiple cells could not be done with this system. The advantage of System III is that with PMT as a detector, a very wide dynamic range is possible, and very weak or very rapid changes in cytosolic calcium concentration could be readily measured.

3.4. System IV

Changes in cytosolic calcium concentration were measured with System IV in both pancreatic acinar cells and hepatocytes. Similar to Systems I and II, with System IV, multiple cells could be measured simultaneously. The stimulation of 10 pM CCK induced regular calcium oscillations, and wash-out of CCK resulted in the disappearance of oscillation (Fig. 5(a) and (c), $n = 6$). The response was similar to that obtained with Systems II and III. PE stimulation of hepatocytes also induced regular calcium oscillations; such oscillations persisted until PE was washed out (Fig. 5(b) and (d), $n = 6$).

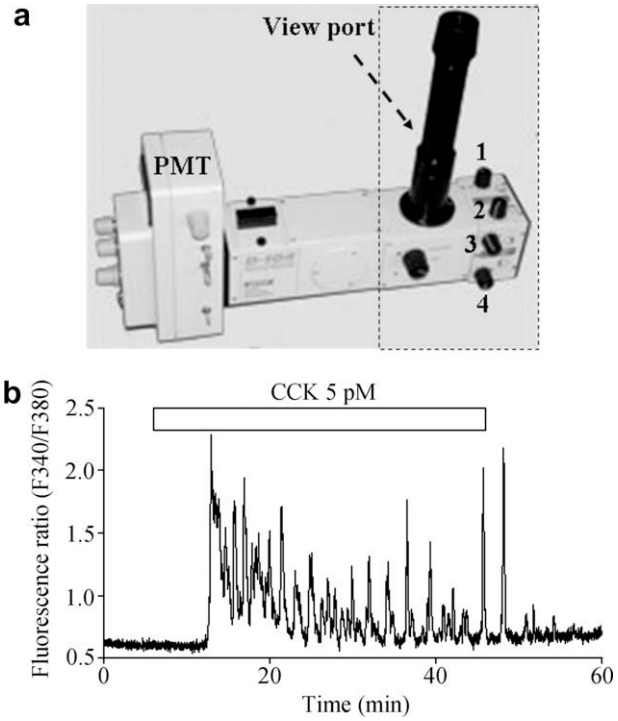

Fig. 4. Oscillatory increases in cytosolic calcium concentration in rat pancreatic acinar cells detected with System III. A pin-hole device was placed in front of the PMT in the light path as indicated by dashed square in (a), ROI was framed by adjusting the four turn-key buttons (indicated as 1–4 in the graph), and could be observed by the naked eye through the vertical view port. Average fluorescence intensity in the square-shaped ROI and fluorescence ratios F340/F380 were measured. The oscillatory calcium concentration increases in a pancreatic acinar cell after stimulation with 5 pM CCK are shown in (b). The horizontal bar indicates time of CCK application. The pin-hole device image in (a) is modified from PTI website: http://www.pti-nj.com/RatioMaster/RatioMaster.pdf.

4. Discussion

CCK-1 is a major secretagogue receptor in pancreatic acinar cells, and low concentration stimulation of CCK-1 receptors triggers persistent cytosolic calcium oscillations. Increase in calcium concentration leads to the synthesis and secretion of digestive enzymes (zymogens) [14,15,20]. Four different equipment setups were used in this paper

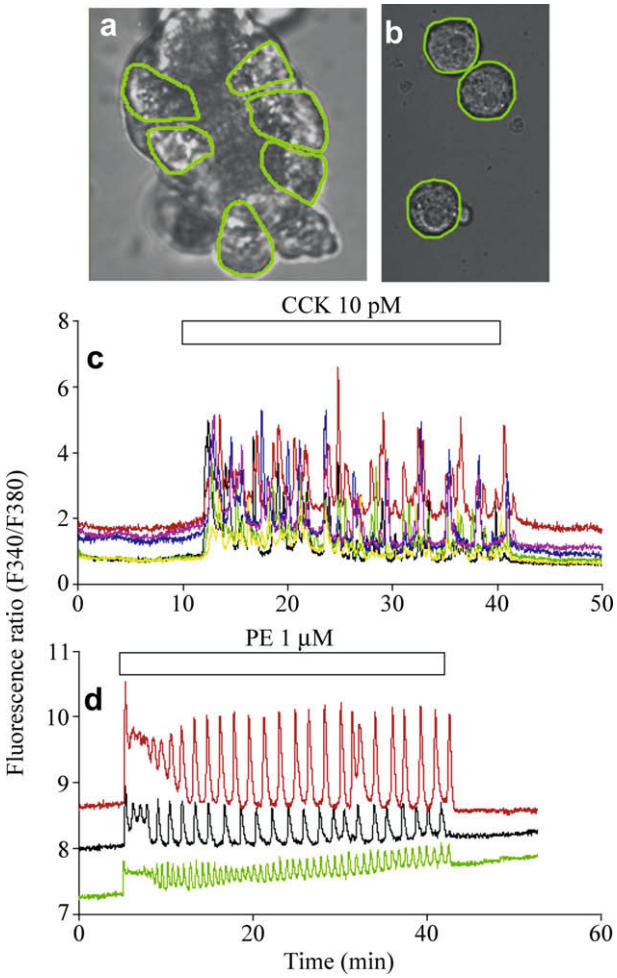

Fig. 5. Oscillatory increases in cytosolic calcium concentration in rat pancreatic acinar cells and in hepatocytes detected in System IV. (a) and (b) Micrographs show transmitted images of pancreatic acinar cells and of hepatocytes. ROIs in green outline individual pancreatic acinar cells (a) and hepatocytes (b). (c) Cytosolic calcium oscillations were induced by 10 pM CCK in ROIs 1–6. (d) Three hepatocytes shown in (b) after stimulation with 1 μM PE all showed oscillatory cytosolic calcium concentration increases. The horizontal bars in (c) and (d) indicate time of drug application.

to detect such calcium oscillations and were all successful. System IV was also used to measure oscillatory calcium increases in hepatocytes, with the results similar to a previous report [19]. With System I, cytosolic calcium oscillations decayed gradually and after a certain time disappeared completely; but such oscillations lasted throughout the experiment with Systems II–IV. In System III, an ROI was selected through a pin-hole device and PMT was used as the detector, therefore only one ROI (or one cell) could be measured at a time; while in Systems I, II and IV, a CCD camera was used; therefore, multiple ROIs or multiple cells could be measured simultaneously.

The light source in System I was a metal halide lamp, whereas it was a xenon lamp in Systems II–IV. The emission spectra of the two types of lamp are shown in Fig. 1(c); the emission from the xenon lamp was continuous, and the strong emission in the UVA region was obvious (Fig. 1(d)); whereas for the metal halide lamp, the major emission peaks were seen at 360, 400, 430, 540, and 570 nm (Fig. 1(c)). With the metal halide lamp, a weak emission was seen at 380 nm, and emission at 340 nm was not available (Fig. 1(c)). The metal halide lamp in Lumen 200 Pro has a power of 200 W, which probably could ensure an adequate output at 340 nm, but the wide bandwidth of the filtered 340 nm light may contain a substantial amount of UVA light <340 nm. Light at the shorter wavelengths may be substantially more toxic than 340 nm to the acinar cells, therefore even during CCK stimulation, calcium oscillations started to decay, and eventually led to a total lack of response for further stimulation with CCK and ACh (Fig. 2(b)). The power output of Lumen 200 Pro could be attenuated at the graded steps of 1% from 0% to 100%. Cellular injury could probably be minimized when the light intensity was further reduced. The Fura-2 excitation light from Lumen 200 Pro was filtered through a filter wheel, the bandwidth of a Fura-2 filter was quite wide (340 ± 25 nm) (see: http://www.chroma.com/). A reduction in the bandwidth of 340 nm output will reduce UVA light below 340 nm. And this could be done by a monochromater with an adjustable slit-width.

The light sources in Systems II–IV are monochromaters. In System II it is Hamamatsu C7773, with emission from 330 to 650 nm. With a xenon lamp (150 W), C7773 power output at 500 nm is 3.5 mW. The slit-width in C7773 is adjustable; thereby, the light intensity can be adjusted. The monochromaters in Systems III and IV are DeltaRam V and DeltaRam X from PTI, with an output slit-width manually adjustable from 0 to 24 nm; therefore, the light intensity could also be adjusted. In this work, the DeltaRam slit-width was set at 1 nm. DeltaRam X had emission from 250 to 680 nm. DeltaRam X power output at 300 nm was 18 mW, and at 473 nm was 19 mW (Allan Stevenson and Xiao Dong Zhang, PTI, personal communications). Both DeltaRam V and X use a xenon lamp (75 W), which emits continuously in the UVA region and the emission is strong (Fig. 1(d)). The monochromaters used in Systems II–IV are all with an adjustable slit-width; thereby, light intensity could be adjusted continuously. In this work, when the DeltaRam slit-width was set at 1 nm, and light intensity was adequate, no cellular damage was noticed (Figs. 4 and 5).

The fluorescent calcium indicator used in this work is Fura-2, therefore high-speed switching of Fura-2 excitation light between 340 and 380 nm is essential for high-speed acquisition of data. The speed of switch between 340 and 380 nm determines the speed of acquisition of the fluorescent ratios F340/F380. In Lumen 200 Pro (Prior Scientific Inc.), the switching between neighboring filters could be completed in 55 ms, a complete cycle for such change could be completed in 110 ms, therefore for imaging the maximum speed for F340/F380 ratio images is 9 frames/s. Hamamatsu C7773 could complete 340/380 nm switching in 3 ms, when coupled with CCD HiSCA, ratio images could be gained at a speed of 80 frames/s. DeltaRam X could complete 340/380 nm switching in 2 ms, a complete cycle could be completed in 4 ms, the speed of detection is determined by the detector. With PMT as the detector, the speed is much higher; with CCD QuantEM 52SC, imaging could be taken at 30 frames/s.

For the measurement of cytosolic calcium concentration, normally an inverted fluorescence microscope is used. Nikon TE-2000U was used in Systems I and IV, Olympus IX71 in System II, Olympus IX70 for System III. Since Fura-2 was used as the fluorescent calcium indicator, a major consideration was UVA transmission (transmission at 340 nm especially) of the microscope objectives. Nikon S Fluor 40× and S Fluor 40× H Superfluo objectives have a transmission at 340 nm of 43% and 52%, respectively, and at 380 nm of 69% and 74%, respectively (Tadashi Iida, Nikon, personal communication). Olympus fluorescence objective UAPO40X/340 has a transmission at 340 nm of 50%, at 380 nm of 75%; UAPO40XOI3/340 at 340 nm of 55%, and at 380 nm of 80% (Jing Jing Qi, Olympus, personal communication). Judging from these parameters it is obvious that such high UVA transmission objectives from Nikon and Olympus meet the requirements for Fura-2 fluorescent detection.

Fluorescence signals can be detected with CCD or PMT. The CCD used in System I is Hamamatsu ORCA-AG, with pixels of 1344×1204. This CCD can be cooled to −30 °C, and the quantum efficiency in the green-red region is 70%. System II is equipped with Hamamatsu CCD ORCA-HR (C4742-95-12HR), with effective pixels of 4000×2624, minimum exposure time of 330 s, quantum efficiency at 460 nm of 50%, cooled to 5–7 °C. System III uses Hamamatsu PMT 1527P (PTI PMT814), its quantum efficiency from 300 to 500 nm is 0.11–0.2 (0.2 at 300 nm, 0.19 at 400 nm, 0.11 at 500 nm, see: http://jp.hamamatsu.com/resources/products/etd/pdf/R1527_TPMS1007E02.pdf). System IV involves the use of Roper Scientific CCD QuantEM512SC, with pixels of 512×512, cooled to −30 °C, with a quantum efficiency of 90%. When high speed and high sensitivity are required, and spatial resolution is not essential, PMT can be used. Both spatial

resolution and quantum efficiency are the major parameters to consider when choosing CCDs. When very weak signals are involved, a high quantum efficiency CCD is needed.

The software used in System I is Simple PCI 6.2, which is user-friendly, and it can automatically store all acquired images, and analyze data. AquaCosmos 2.5 is used in System II, Felix 1.42b is used in System III (the most updated version is now Felix 32). Since no images are stored in System III, the computer hard-disk need not be very large. System IV is operated with software EasyRatioPro. System IV is unique in that an ergonomic WarpDrive makes operating the system very comfortable and easy, without the need to use the mouse for complex windows operations.

System III is the only system with PMT as the detector. The advantage with PMT is its high sensitivity and detection of very weak signals, and a wide dynamic range. The disadvantage is that each time only a single ROI can be measured; once the ROI is selected, it cannot be changed during the course of the experiment. In contrast, with imaging, multiple ROIs can be measured (different cells or different regions within the same cell). Fig. 2 illustrates that with System I, average calcium concentration in the whole cell, in the basal portion, in the apical portion could all be measured simultaneously. The oscillatory frequency in the three ROIs was completely identical. However, the calcium spike amplitude was not identical: it was high in the basal portion, low in the apical portion; and the whole cell average was in between. In pancreatic acinar cells, zymogen granules are enriched in the apical region, whereas endoplasmic reticulum is enriched mainly in the basal region. Such polarity determined that calcium signal amplitude was also polarized. Note that in System I decay and disappearance of CCK-induced calcium oscillations could be because of over exposure of UVA light at $<$340 nm. Attenuation of light strength could potentially solve this problem of cell injury.

With System II, multiple ROIs could also be measured simultaneously, to compare the differences in calcium signals in different cells and different regions in the same cell. The pseudo-color calcium ratio images for multiple ROIs could be seen online during the measurement, therefore calcium concentration changes in different ROIs could be seen directly during the measurement. A maximum of 10 ROIs could be measured simultaneously with System II, but no ROI could be drawn within a larger ROI. Therefore, it was not possible to compare the whole cell average and local calcium concentration within the same run of the experiment. However, a bigger or smaller ROI could be drawn and analyzed after all image data have been stored and re-analyzed.

With System IV, the number of ROIs is not limited, smaller ROIs could be drawn within larger ones; furthermore, new ROIs could be added anytime during the course of the experiment. Fig. 5 illustrates that when CCK was added to the pancreatic acinar cells, or when PE was added to hepatocytes, regular cytosolic calcium oscillations appeared. The basal fluorescence ratios F340/F380 were quite uniform in different pancreatic acinar cells, whereas such basal ratios were rather different among different hepatocytes. This indicates that the basal calcium concentration is uniform among pancreatic acinar cells, but not among hepatocytes. After a low level stimulation, both cell types showed regular calcium oscillations. The purpose-built computer in System IV ensures that all image data could be stored in real time on the computer hard disk. The software EasyRatioPro still has room for further improvements. During an ongoing experiment, the images (F340, F380, or F340/F380) could be shown only in sequence in a single window, not simultaneously in multiple windows. It would be better if in future versions the three images could be shown in three separate windows. This is also the case for fluorescence intensity plots. F340, F380, and F340/F380 are presently plotted online in a single window; different magnitudes of the values make simultaneous display of fluorescence intensities and ratios impossible. F340, F380, and ratio F340/F380 should really be shown in two separate windows, in which the simultaneous displays of both intensity and ratio will be realized.

In summary, the following should be considered when a calcium measurement/imaging system is to be purchased: a xenon light source is preferred, if high frequency measurement is not essential, a filter wheel device could be chosen which is economical. If high-speed acquisition is essential, a special monochromater is imperative, preferably with an adjustable output slit-width. For measurement with Fura-2 as the calcium indicator, special consideration should be made in regards to UV transmission at 340 nm for the microscope objectives. Spatial resolution and quantum efficiency of the CCD are two important parameters to consider. For the detection of ultra-weak signals, higher quantum efficiency is recommended. The data acquisition and analysis software should be ergonomic, and user-friendly, whereby real-time display of signal, multiple modes of data storage such as images, text data, and pseudo-color display are made possible. For imaging experiments, a large hard disk or special storage devices are essential.

In this paper, we have mainly discussed equipment setups for Fura-2 detection. When single wavelength fluorescent indicators such as Fluo-3 are used, only one excitation wavelength is used. For fluorescent calcium imaging, the single wavelength excitation, dual wavelength emission-probe Indo-1 can also be used. Because only a single excitation wavelength is needed (350 nm) with Indo-1, high-speed switching between excitation wavelengths is not required for the light source; therefore, a less expensive light source could probably be used. However, it is best if the bandwidth of the excitation wavelength is adjustable. With Indo-1, detection of two emission wavelengths is required. For example, in System III above, two PMTs will be needed. Emitted light is split by a dichroic mirror (and two emission filters for 390 and 475 nm, respectively) in the light path before PMT into 390 and 475 nm, with

two PMTs each detecting the two emission wavelengths, respectively, to get fluorescent ratios F390/F475. For fluorescent calcium ratio imaging, a "dual view" image splitting device (see: http://www.magbiosystems.com/products/multichannel.php) is used to split the fluorescent image into two simultaneous images. Either two separate CCDs are used (with splitting device DC2), or a single CCD is used (with splitting device DV2) to get the ratio fluorescent images F390/F475 nm.

Acknowledgments

Parts of the experiments with Systems I and II were performed during a workshop on Modern Microscopic Imaging and Applications in Biomedical Research organized by The Institute of Biophysics CAS and Hamamatsu Medical University Japan during 13–16 May 2007. Work in the authors' laboratory was supported by the National Natural Science Foundation of China (Nos. 30472048, 3054042524, and 30728020) and NSF Beijing (No. 6062014). Equipments were provided by Hamamatsu KK, Nikon Inc. and Olympus Inc. during the workshop.

References

[1] Winslow MM, Crabtree GR. Decoding calcium signaling. Science 2005;307:56–7.
[2] Knot HJ, Laher I, Sobie EA, et al. Twenty years of calcium imaging: cell physiology to dye for. Mol Interv 2005;5:112–7.
[3] Su L, Ma CY, Zhou YD, et al. Cytosolic calcium oscillations in the submandibular gland cells. Acta Pharmacol Sin 2006;27:843–7.
[4] Xu X, Hotta CT, Dodd AN, et al. Distinct light and clock modulation of cytosolic free Ca^{2+} oscillations and rhythmic CHLOROPHYLL A/B BINDING PROTEIN2 promoter activity in *Arabidopsis*. Plant Cell 2007;19:3474–90.
[5] Pang X, Halaly T, Crane O, et al. Involvement of calcium signalling in dormancy release of grape buds. J Exp Bot 2007;58:3249–62.
[6] Campbell AK, Naseem R, Holland IB, et al. Methylglyoxal and other carbohydrate metabolites induce lanthanum-sensitive Ca^{2+} transients and inhibit growth in *E. coli*. Arch Biochem Biophys 2007;468:107–13.
[7] Trimble WS, Grinstein S. TB or not TB: calcium regulation in mycobacterial survival. Cell 2007;130:12–4.
[8] Nikolskaia OV, de A Lima AP, Kim YV, et al. Blood–brain barrier traversal by African trypanosomes requires calcium signaling induced by parasite cysteine protease. J Clin Invest 2006;116:2739–47.
[9] Cheshenko N, Liu W, Satlin LM, et al. Multiple receptor interactions trigger release of membrane and intracellular calcium stores critical for herpes simplex virus entry. Mol Biol Cell 2007;18:3119–30.
[10] Grant JR, Moise AR, Jefferies WA. Identification of a novel immunosubversion mechanism mediated by a virologue of the B-lymphocyte receptor TACI. Clin Vaccine Immunol 2007;14:907–17.
[11] Motta PM, Macchiarelli G, Nottola SA, et al. Histology of the exocrine pancreas. Microsc Res Tech 1997;37:384–98.
[12] Cui ZJ, Kanno T. Photodynamic triggering of calcium oscillations in the isolated rat pancreatic acini. J Physiol (Lond) 1997;504:47–55.
[13] Petersen OH, Burdakov D, Tepikin AV. Polarity in intracellular calcium signaling. Bioessays 1999;21:851–60.
[14] An YP, Xiao R, Cui H, et al. Selective activation by photodynamic action of cholecystokinin receptor in the freshly isolated rat pancreatic acini. Br J Pharmacol 2003;139:872–80.
[15] Xiao R, Cui ZJ. Mutual dependence of VIP/PACAP and CCK receptor signaling for a physiological role in duck exocrine pancreatic secretion. Am J Physiol 2004;286:R189–98.
[16] Rooney TA, Joseph SK, Queen C, et al. Cyclic GMP induces oscillatory calcium signals in rat hepatocytes. J Biol Chem 1996;271:19817–25.
[17] Woods NM, Cuthbertson KS, Cobbold PH. Repetitive transient rises in cytoplasmic free calcium in hormone-stimulated hepatocytes. Nature 1986;319:600–3.
[18] Cui ZJ, Habara Y, Satoh Y. Photodynamic modulation of adrenergic receptors in the isolated rat hepatocytes. Biochem Biophys Res Commun 2000;277:705–10.
[19] Cui ZJ, Guo LL. Photodynamic modulation by Victoria Blue BO of phenylephrine-induced calcium oscillations in the freshly isolated rat hepatocytes. Photochem Photobiol Sci 2002;1:1001–5.
[20] Williams JA, Sans MD, Tashiro M, et al. Cholecystokinin activates a variety of intracellular signal transduction mechanisms in rodent pancreatic acinar cells. Pharmacol Toxicol 2002;91:297–303.